

# Forecasting Generalized Epileptic Seizures from the EEG Signal by Wavelet Analysis and Dynamic Unsupervised Fuzzy Clustering

Amir B. Geva,\* *Member, IEEE*, and Dan H. Kerem

**Abstract**—Dynamic state recognition and event-prediction are fundamental tasks in biomedical signal processing. We present a new, electroencephalogram (EEG)-based, brain-state identification method which could form the basis for forecasting a generalized epileptic seizure. The method relies on the existence in the EEG of a pre-seizure state, with extractable unique features, *a priori* undefined.

We exposed 25 rats to hyperbaric oxygen until the appearance of a generalized EEG seizure. EEG segments from the pre-exposure, early exposure, and the period up to and including the seizure were processed by the fast wavelet transform. Features extracted from the wavelet coefficients were inputted to the unsupervised optimal fuzzy clustering (UOFC) algorithm.

The UOFC is useful for classifying similar discontinuous temporal patterns in the semistationary EEG to a set of clusters which may represent brain-states. The unsupervised selection of the number of clusters overcomes the *a priori* unknown and variable number of states. The usually vague brain state transitions are naturally treated by assigning each temporal pattern to one or more fuzzy clusters.

The classification succeeded in identifying several, behavior-backed, EEG states such as sleep, resting, alert and active wakefulness, as well as the seizure. In 16 instances a pre-seizure state, lasting between 0.7 and 4 min was defined. Considerable individual variability in the number and characteristics of the clusters may postpone the realization of an early universal epilepsy warning. Universality may not be crucial if using a dynamic version of the UOFC which has been taught the individual's normal vocabulary of EEG states and can be expected to detect unspecified new states.

**Index Terms**—EEG, fuzzy clustering, hyperbaric oxygen, rat, temporal pattern recognition, time-frequency analysis.

## I. INTRODUCTION

**H**UMAN epilepsy is, for the most part, an intrinsic brain pathology. Its major manifestation is the epileptic seizure which may involve a discrete part of the brain (partial) or the whole cerebral mass (generalized). In the latter instance, seizures or ictal states are recurrent, with interictal periods ranging from several minutes to many days. Ictal electroencephalogram (EEG) is characterized by repetitive high-amplitude activity, either fast (spikes), slow (waves),

or spike-and-wave (SPW) complexes. This activity varies, depending on the type of epilepsy. It may take the form of 2–60-s periods of very regular and symmetric 3-Hz SPW discharges in *absence* or *petit mal* epilepsy. The *tonic-clonic*, or *grand mal* epilepsy, has 40–60-s periods with fast polyspike activity, gradually decreasing in frequency and increasing in amplitude (tonic phase) interrupted by slow waves (clonic phase), and followed by post-ictal EEG depression. Other less regular patterns occur in *myoclonic*, *clonic*, *tonic*, *atonic*, and *atypical absence* epilepsies [1].

The EEG in the interictal periods ranges from normal, through isolated epileptic activity (single events or brief bursts) riding on a normal background, to an abnormal background (usually slow) with or without riding isolated epileptic activity. Other than frank paroxysmal activity such as spikes or SPW complexes, the riding events may include single short transients, such as abnormal rhythms, sub-clinical discharge patterns, and nonparoxysmal complexes [2]. Allusion to a preictal period is sometime made, but usually as an after-sight. While abnormal interictal EEG patterns may sometimes abound just before the seizure, more often than not, the latter strikes unheralded with a dramatic sharp transition of the EEG signal from its ongoing background pattern into the characteristic impulse-train of spikes or (SPW) complexes, coincidental with the motor involvement.

Alerting a patient and/or his attending staff to an impending epileptic seizure has obvious clinical importance. The above-described changes in the EEG make this signal an intriguing candidate for a forecaster. Yet, in spite of a massive invasion of signal-processing expertise into the field of neurology, and in spite of considerable effort invested in detecting epileptic patterns, an early (few minutes) and reliable universal forecaster has yet to be found.

There is one population of individuals with intact cerebral function, in which generalized *grand mal*-type epilepsy may be inadvertently and reversibly induced by external means. These are individuals that breath oxygen at an increased ambient pressure [hyperbaric oxygen (HBO)], either while diving with closed-circuit breathing apparatus or while receiving treatment inside a pressure chamber. The elevated oxygen partial pressure, by mechanisms not completely elucidated, induces generalized EEG seizure patterns as well as motor convulsions after a time delay which gets shorter as the pressure gets higher [3]. These subjects may best benefit from an alarm system, yet, having no chronic pathology, we cannot provide

Manuscript received February 19, 1997; revised April 16, 1998. This work was supported in part by the Israel Science Foundation, founded by the Israel Academy of Sciences and Humanities. Asterisk indicates corresponding author.

\*A. B. Geva is with the Electrical and Computer Engineering Department, Ben Gurion University of the Negev, P.O. Box 653, Beer Sheva 84105 Israel.

D. H. Kerem is with the Israeli Naval Medical Institute, IDF Medical Corps, P.O. Box 8040, Haifa 31080 Israel.

Publisher Item Identifier S 0018-9294(98)06951-1.

the individualized pre- or interictal EEG information upon which to base such an alarm.

Apart from its practical uses, HBO provides a very valuable experimental model. The animal model used in this study is a chronically implanted unrestrained rat. Exposure of the experimental animal to HBO will bring about seizures after a predictable mean time lag, ranging from a few hours to a few minutes, depending on exposure pressure [3]. Sometime during the 5 min preceding the first major (>20-s) electrical discharge in the EEG there is very often a state of alertness with the animal expressing escape behavior. This fact may hint that a preictal state (PIS) indeed exists in generalized epilepsy, which is sensed by the rat but not by most patients. EEG records of human subjects in whom HBO-induced seizures occurred are very rare. Thus, the readily available EEG records from HBO-exposed rats, up to and including the first seizure, are a good data bank to try to universally define the PIS and, by so doing, to forecast the seizure.

The EEG record during the PIS should be searched for abnormal isolated activity as well as for nonparoxysmal changes in background activity. Indeed, a gradual change in the state of the cortex may be required for single events (normally suppressed) to evolve into a full-blown seizure [4]. Such changes may be apparent from information contained in a single derivation or only from information contained in two or more.

Both for the clinical and for the operational application, a universal, automated feature-extraction system is needed which will detect the ictal state (IS) with a high degree of sensitivity and specificity. The detection should be achieved at an early enough stage, especially in the operational arena, so that proper action may be taken in order to avert the impending seizure. A host of signal processing methods have been put forward for application to pre- or interictal EEG, both for classification following parameter extraction and for supervised pattern recognition [2], [4]–[21]. Several specific attempts at epilepsy prediction have been made, both on experimental animals and human epileptic patients [22]–[29]. Of those based on sharp-transient detection, the few successful ones lacked universality, being reliant on prior familiarity with the individual's seizure discharge patterns [23], [26]. Some attempts, which tracked nonspecific changes in background activity, found them too close (a few seconds) to the seizure to be practical [24], [27]–[29].

Since the PIS may be defined by single or short-lasting events as well as by dynamic changes in background activity, and since paroxysmal-like single events may appear during states unrelated to the epileptic seizure, a signal processing method capable of dissecting and categorizing the pattern of short EEG epochs is needed. The epochs need be short so as to be sensitive to rapid transients but long enough to capture the underlying state of the cortex. A dynamic categorizing process which takes into account all past history of the signal is vital for a forecasting process which needs to recognize a change in pattern not only at that time, but in the long perspective of all seizure-unrelated patterns.

We can take advantage of the fact that (patho) physiological states of the brain are very often characterized by distinct

combinations of the basic EEG rhythms. An EEG state can be defined by a portion of the time-series dominated by one rhythm, a particular mixture or alternation of rhythms, or the frequent appearance of isolated events. If we pool the values of a properly chosen combination of parameters produced over time by some feature extracting method, they would be expected to be naturally classifiable into groups representing such states.

A clustering procedure allows state classification by taking account of past history. Unlike segmentation, clustering classification, by making use of past data, can distinguish between “normal” state-changes and a change into a true new state. Notwithstanding the distinct rhythms, temporal pattern variation in the EEG time-series is a continuum and the emergence of a new state may not always be sharp. Thus, attempting to classify the multidimensional space points into discrete, nonoverlapping categories will leave much of the content unclassified or classified by default. The method of fuzzy clustering overcomes this by allowing items to share membership in more than one category. A state could, thus, be defined not only by the cluster list representing it but also by the degree of membership in various clusters.

By not forcing *a priori* constraints on cluster features, the unsupervised optimal fuzzy clustering (UOFC) algorithm [31]–[32] gains flexibility to detect changes not entirely foreseen. For instance, the number of clusters could be dictated according to the maximal number of different normal EEG states seen in the unrestrained rat. However, by allowing the clustering procedure itself to decide, by certain validity criteria, on the optimal number of clusters for any given categorization, we may guard against an artificial grouping in sequences which do not include all normal rhythms and states. The optimal number of clusters, their spatial location, and the membership therein of each data point are all obtained by unsupervised learning during the classification of each individual case.

The UOFC may be used in two ways (or their combination) for automated definition of EEG states. The first is by application to EEG sequences, which include sufficiently long segments representing the “normal” repertoire of patterns (backed by behavioral signs) as well as clinical states. Abnormal patterns or combinations, associated with chronic pathology or heralding an acute pathological event, will be expected to form distinct classes. This is the means better suited for determining the usefulness of the method and is the main one to be described in this paper.

The second means, which better serves an actual automated forecasting device, is to have the procedure operate from the beginning of an exposure expected to lead to pathology, and to observe the dynamics of the classification as consecutive data are being introduced. A combination of adaptive, on-line, classification and the use of past information can be achieved by applying a weighting function to the time series. An abrupt and considerable change in the optimal number of classes, in the validity criteria of a given number of classes, and in the spatial shift of one or more cluster centers could, together, signal the advent of a new state in general and of an epileptic state in particular.

This paper is the culmination of a lengthy quest for a signal processing tool which can best detect the PIS and forecast the seizure in experimental HBO-induced epilepsy. The general approach was to couple feature extraction with UFOC as the categorization tool of selected transform coefficients. This approach was found successful, using adaptive segmentation as the feature extractor, in identifying general EEG states [30] as well as EEG segments containing “significant graphoelements,” such as epileptic bursts [21]. We have tried various processing modes in an effort to define the PIS and forecast the seizure. After failing to confirm consistent spectral changes in the PIS [25] using the short fast Fourier transform (FFT), we have tried adaptive segmentation by linear prediction [24], the auto-correlation function, and matching pursuit (33), all on a single EEG channel, and also changes in co-correlation and coherence functions of bi-channel signals. Although some of the methods succeeded in forecasting seizures, we found the parameters produced by the wavelet transform of two channels, to be superior to all others we have tried, judged by the percentage of successful forecasts.

The results of applying the “static” classification mode on records from 25 animal exposures and the “dynamic” mode on five of the same, make us believe that a PIS does exist in this model and is amenable to detection and definition. While the attainment of the desired automated forecaster in the model, and certainly in wider clinical usage, will need further refinement of the method, we believe that it is a path well worth pursuing.

## II. METHODS

### A. Data Acquisition

HBO-induced generalized seizures were obtained by exposing laboratory rats implanted with chronic surface cortical electrodes to pure oxygen in a pressure chamber. Rats were at least four days post operative, resting-unanesthetized and unrestrained. Two bipolar channels of EEG, fronto-frontal and parieto-parietal, were amplified, filtered to pass between 1 and 30 Hz (−6 dB/octave), notch-filtered at 50 Hz (−20 dB/octave), and recorded on paper and tape. After a period of accustomization to the chamber, five minutes of control EEG, breathing oxygen at normal pressure, were recorded. Recording was halted for five minutes of compression to 5-atm-abs pressure, and then resumed until the appearance on the chart paper of the first major (>20 s) seizure which prompted decompression. Some animals were exposed twice, after a period of at least three days.

The replayed tape recordings were digitized at a sampling rate of 128 Hz. Four-minutes of control (C) EEG, four minutes of early pressure exposure, and the last five minutes prior to and including the seizure were divided into consecutive 1-s epochs. In some short exposures, the pressure (P) and pre-seizure (PS) periods were continuous.

The epoch-divided sections of each channel of the EEG signal  $S(n), n = 1, \dots, (M-1) \cdot D + N$  were arranged as the columns (pattern vectors) of an  $N \times M$  matrix  $\mathbf{S}$ , where  $N$  is the dimension (number of samples) of each pattern vector,  $M$

is the number of patterns, and  $D$  is the delay between patterns

$$\mathbf{S} = \begin{bmatrix} S(1) & S(D+1) & \cdot & \cdot & S((M-1) \cdot D + 1) \\ S(2) & S(D+2) & \cdot & \cdot & S((M-1) \cdot D + 2) \\ \cdot & \cdot & \cdot & \cdot & \cdot \\ \cdot & \cdot & \cdot & \cdot & \cdot \\ S(N) & S(D+N) & \cdot & \cdot & S((M-1) \cdot D + N) \end{bmatrix}.$$

In our realization, we chose  $N = 128$  samples (1-s) and  $D = N/2$  (overlap of half of the samples between consecutive pattern vectors). Such short and overlapped windows ensure that all transient events will be completely represented and dominant in at least one of the patterns. Yet, they are long enough to characterize the main “rhythms” (between 2 and 30 Hz) of the on-going EEG signal. The feature extraction procedure, to be described in Section II-B, was applied to the columns of  $\mathbf{S}$ .

### B. Multiscale Decomposition by the Fast Wavelet Transform (FWT)

The wavelet transform provides an important tool in signal analysis and feature extraction [19], [20], [34], [35]. It produces a good local representation of the signal in both the time domain and the frequency domain. Unlike the Fourier transform, which is global and provides a description of the overall regularity of signals, the wavelet transform looks for the spatial distribution of singularities. This transform suits the EEG signal which is not stationary by its nature, has time-variant frequency content, and contains normal singular events such as the  $k$ -complexes and sleep spindles, as well as abnormal ones such as spikes and SPW’s. The wavelet transform can accommodate transients in contrast to the Fourier transform which assumes signal stationarity.

In this paper, the FWT, proposed by Mallat and Zhong [34], is applied (for details, see Appendix A). Each column of the time series matrix  $\mathbf{S}$  is decomposed into an orthogonal set of waveforms that are the dilations, translations, and modulations of a single biphasic wavelet (mother wavelet). The FWT with the simple biphasic mother wavelet was chosen because the latter fits the biphasic nature of the EEG signal and the epileptic complexes (see Fig. 1), and in practice showed better results than other common wavelet bases that we tested. The wavelet transform is computed by convolving the signal  $S$  with these dilated wavelets. The wavelets’ coefficients of the different scales,  $T_{2^j} \mathbf{S}, j = 1, \dots, J$  ( $J$  is the number of scales), offer a compact representation of the EEG signal, as seen in Fig. 1.

The number of scales should be chosen by the spectral content of the signal. It has been demonstrated [35] that scales higher than the first five (roughly conforming to the principal EEG rhythms) do not add significant information about the EEG signal. For each scale, the statistical values of the moments of variance (energy), skewness, and kurtosis of the wavelet coefficients are computed. Also computed are the correlations between wavelet coefficients of each and the other scales. In addition to the above statistics, the number of extrema (zero crossings) per unit time in the transform, which contains other relevant information about the signal, are obtained (Fig. 1) and added to the list of possible inputs

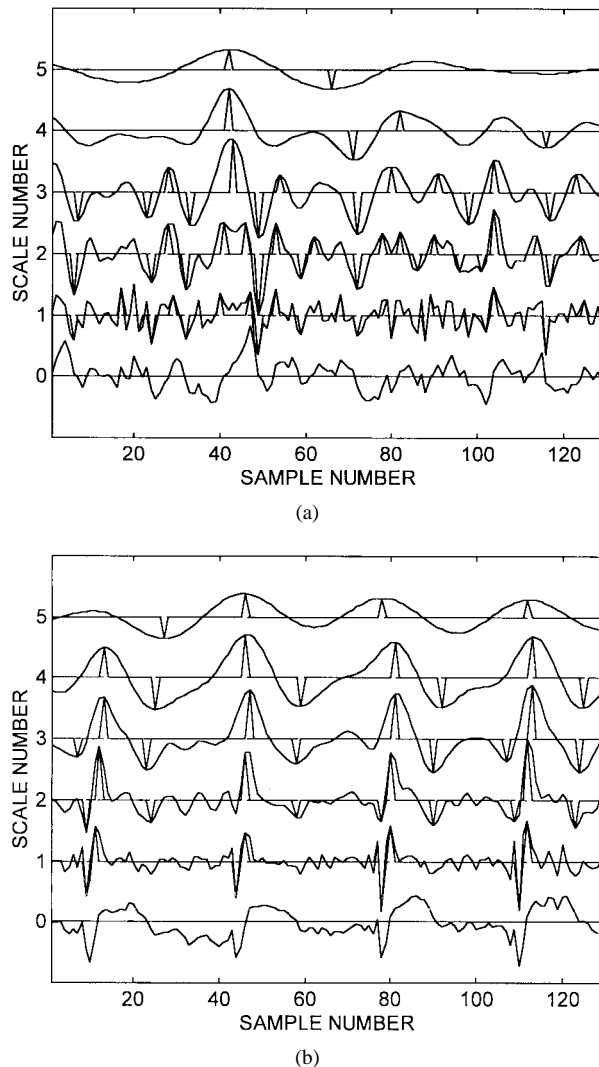


Fig. 1. Examples of wavelet transforms of 1-s EEG epochs. The original signal is shown at the bottom of each panel and above it are the successive scales of the wavelet coefficients. It is evident that the transform involves differentiation and progressive smoothing. The major peaks (zero crossings of the signal) which survived the thresholding process are also marked. These peaks are sufficient to reconstruct the relevant time-frequency content of the original signal. (a) An awake state with  $\beta$  rhythm (30 Hz) riding on  $\theta$  rhythm (6–7 Hz). The  $\beta$  rhythm is picked-up by the first scale only, the slower  $\theta$  by scales 3 and 4. Events such as the steep rise of the third  $\theta$  wave are evident on all scales but scale 5 seems superfluous. (b) A fully developed seizure with 5-Hz SPW complexes. Information about the spike is contained in scale 1, which only detects the steep rise of the wave. Details of the spike are gradually lost as the downward slopes of the wave are being picked up at higher scales.

to the clustering. These statistical values then serve as the extracted features to form the column vectors of the  $F \times M$  feature matrix  $\mathbf{X}_F$  for the UOFC algorithm.

### C. The Unsupervised Optimal Fuzzy Clustering (UOFC) Algorithm

The  $\mathbf{X}_F$  features matrix can be directly used as the input to the clustering procedure or can be reduced by the Karhunen–Loeve transform (KLT) [37]. Each column of this matrix is an input pattern to the clustering algorithm. The number and nature of the coefficients chosen for the clustering was determined by trial and error, searching for the minimum that

would succeed in categorizing the observed states including the preictal (the last 4–5 min prior to the seizure).

The clustering is utilized in order to find matching groups within the features matrix. When clustering temporal patterns of the EEG signal, we obtain a nonuniform selection of similar patterns which may allude to different bioelectrical states of the brain. Studying the dynamics of these states may help predict the evolution of the bioelectrical brain activity. Clustering of the coefficients was performed by UOFC, as introduced by Gath and Geva [31], [32], which partitions the data by a combination of the fuzzy  $k$ -means [36] and maximum-likelihood estimation (MLE) algorithms. The superiority of the fuzzy  $k$ -means algorithm, with respect to speed of convergence, is realized by having it compute the cluster centers. These are then fed as initial values for the MLE algorithm which better deals with unequal cluster features.

The advantage of the UOFC algorithm is the unsupervised initialization of cluster prototypes, and the criteria for the number of clusters based on performance measures for cluster validity using fuzzy hypervolume and density functions. It performs well in a situation of large variability of cluster shapes, densities, and number of data points in each cluster. The general scheme of the UOFC algorithm is iterated for an increasing number of clusters in the data set, calculating a new partition of the data set and computing performance measures in each run, until the optimal number of clusters is obtained (see Appendix B for details)

- 1) Choose the initial cluster prototype at the mean location of all data patterns.
- 2) Calculate a new partition of the data set by the following two phases:
  - a) cluster with fuzzy  $K$ -means with an Euclidean distance function.
  - b) cluster with fuzzy  $K$ -means with an exponential distance function; a fuzzy modification of the MLE.
- 3) Calculate performance measures for cluster validity.
- 4) Add another cluster prototype equally distant (with a large given number of standard deviations) from all data points.
- 5) If the number of clusters is smaller than a predecided maximum of clusters, go to Step 2).
- 6) Else, stop and choose the optimal partition by the performance-measure criteria.

Applying wavelet analysis to baseline EEG stretches of many animals, then tracking clustering-optimization criteria (Appendix B) as cluster number progressively increased and, finally, partitioning stretches that included the seizure with different numbers of clusters, showed that the optimal partitioning for accommodating the normal as well as the epileptic EEG states, is obtained by the number of clusters which maximizes the average density (AD) criterion, plus one or sometimes two

$$K_{\text{optimal number of clusters}} = \arg\{\max_K \{V_{AD}(K)\}\} + 1.$$

Accordingly, we added one to the global maximum of the average density criterion to obtain the optimal number of clusters for partitioning the EEG-data of each exposure.

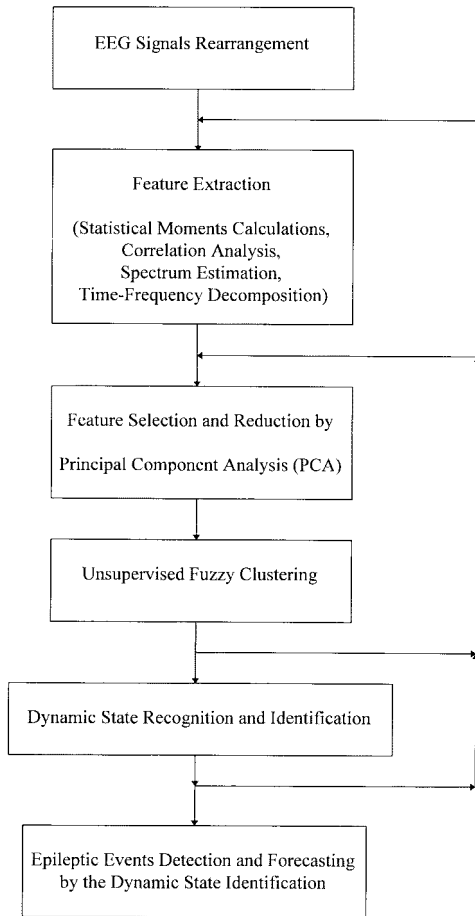


Fig. 2. Block diagram of the procedure of unsupervised fuzzy clustering in forecasting epileptic events from EEG signals. Back arrows signify optional re-selection and/or reverting to other methods of feature extraction, and reduction by the results of clustering and/or state recognition.

We also used this optimal number ( $K_{\text{optimal}}$ ) in a pilot attempt at dynamic tracking of the clustering process. Instead of feeding all data points at once, the classification to  $K_{\text{optimal}}$  clusters was initialized on the first 2.5 min (300 pattern vectors) and then proceeded at consecutive steps of 30-s (60 pattern vectors)-long stretches of signal. The temporal changes in the position of cluster centers and in the magnitude of the average density criterion were then followed.

Fig. 2 is a flow chart of the complete procedure.

### III. RESULTS

During the control period in the chamber and during the HBO exposure, animals alternated between states of sleep, restful wakefulness, attentive alertness, as well as grooming, sniff-searching, and other active states. In many instances, single or groups of spikes, usually accompanied by facial or other muscle twitches, were seen in the EEG during the PIS. Yet, in others the electric seizure seems to spring “out of the blue (or rather gray).” During the first electric discharge, the animal appeared immobile and dazed, similar to *absence*-type *petit mal* seizures in humans. If the exposure were not terminated at this stage, a massive *grand mal* seizure with

tonic-clonic motor involvement would usually ensue after 2–3 min.

Out of 25 exposed animals, one did not have a seizure throughout 65 min (at this time, the exposure was terminated due to early signs of pulmonary oxygen toxicity). The group’s mean seizure time ( $T_s$ ) at this pressure was 16.6 min, the range being 7 to 55 min. Eight of the rats did not show obvious visual signs in the EEG during the PIS (Table II).

The wavelet coefficients, which when fed to the clustering procedure gave the best definition of normal and pathological states and the highest percent of PIS definition, were the combined variances (energies) of the first four scales of the two channels (eight parameters in all). In some animals, mainly for technical reasons, single-channel variances gave slightly better results but for the most part, no channel alone could reach as clear a definition of the PIS as could their combination. Transient (mainly movement) artifacts, which tended to concentrate at the PIS when the animal was very active, could influence classification. The 25 recordings we have picked were as artifact-free as practically possible, in at least one channel. These artifacts may be part of the reason why single-channel parameters sometimes performed better than dual-channel. Other coefficients, which when added or substituted for the variances, sometimes improved PIS identification, were the number of extrema, the mean energy per peak (variance divided by the number of extrema), and the intrachannel correlation of scales 1 and 3. Since in other instances prediction was worse or altogether lost, the final outcome did not warrant their inclusion in a universal input to the UFOC.

Fig. 3(a) shows a three (out of eight)-dimensional (3-D) presentation of a five-cluster classification of all points in a concatenated stretch of EEG, with each point connected to the center of the cluster in which it has the highest degree of membership. The centers are surrounded by ellipses, the radii of which are the standard deviations of the point distances in the three dimensions. Since most of the background energy content of the awake-state EEG resides in the low-amplitude higher frequencies, with the high-amplitude single events being rather rare, the clustering usually proceeded in order of increasing variances of all scales. In this case, there being a rather lengthy sequence of a high-amplitude sleep state which lasted the entire control period, its representative cluster number 2 (see below) stands outside this order.

It is rather obvious that many points share membership in more than one cluster. This fuzziness of the clusters is quantified in Fig. 3(b), which, for each successive point in the time series, plots the degree of membership in each of the clusters (the space between two  $y$ -axis integers equals 100% membership). While there are sequences with a clear predominance of a certain cluster, there are others with points sharing membership in as many as four different clusters.

Matching periods with a temporal preponderance of a given cluster (a time sequence of consecutive points having close to 100% membership in this cluster) to their counterparts in the original signal, we found that in most animals such periods could be correlated with a distinct behavioral and electroencephalographic state, in at least one channel. An ex-

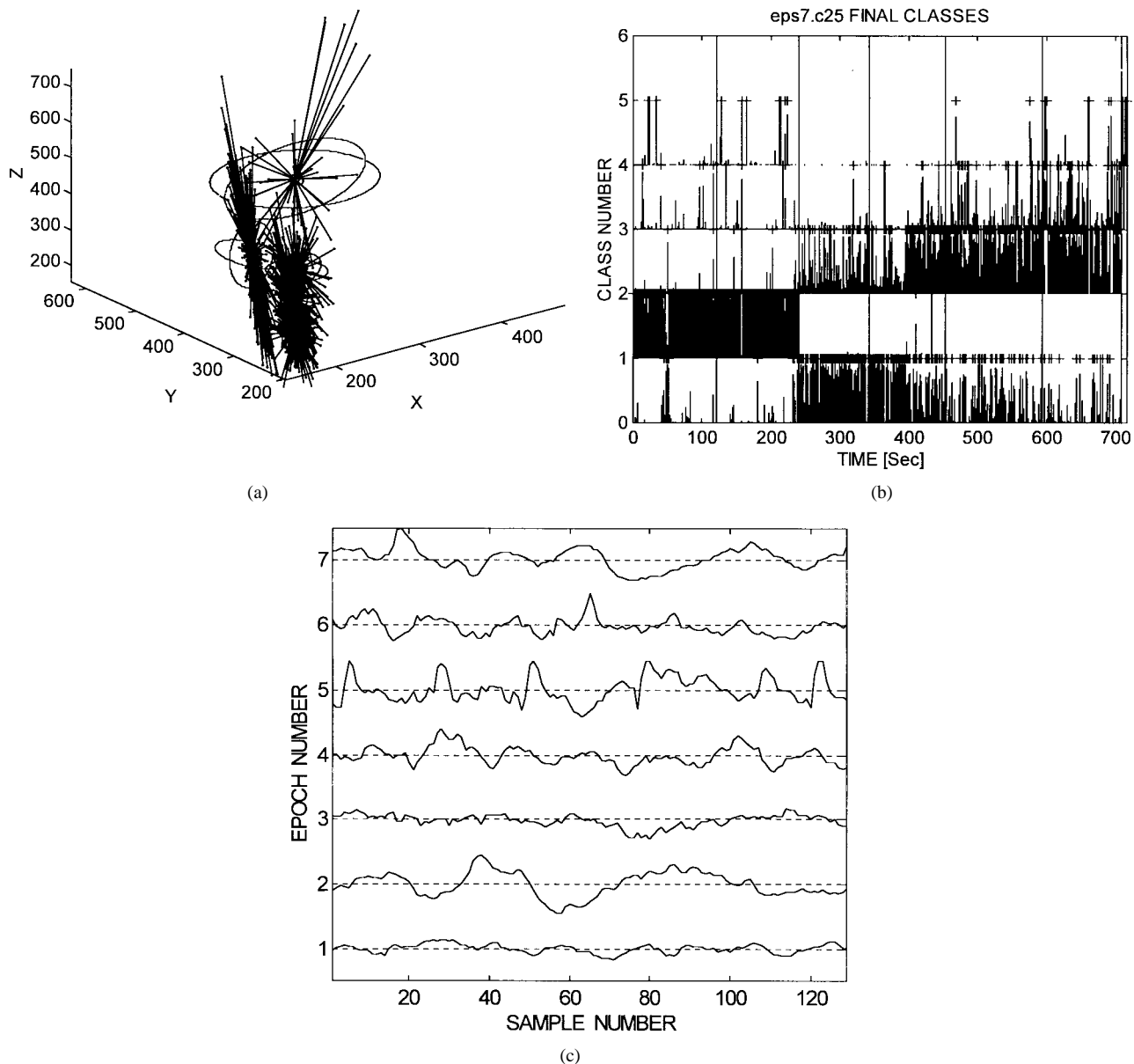


Fig. 3. EEG states (of a rat) categorized by the combined wavelet transform and the UOFC procedure. (a) Clustering results: A 3-D projection of a five-cluster partitioning of a concatenated EEG stretch. The actual partitioning is based on the variances (energies) of the first four wavelet scales of two EEG channels. (b) Degree of membership as a function of time: The Y-axis is the cluster number from (a), the space between integers being equal to 100% membership. The X-axis is time in seconds. Bold vertical lines mark the borders of (from left to right) two control segments (C1 and C2), two segments at early and mid part of pressure exposure (P1 and P2), and lastly, two pre-seizure segments (PS1 and PS2). Beginning of seizure (as located by a human expert) is marked by a bolder line at 710s, in PS2. (c) Corresponding States: Single-channel 1-s epochs of the original signal. The first five epoch numbers correspond to the matching cluster number in (a) and (b). The additional last two epochs (6 and 7) include single events which divide their membership between two clusters (see text for state description).

ample is presented in Fig. 3(c), which illustrates representative single-channel 1-s epochs, taken from periods with a clear predominance of a given cluster: 1 = resting wakefulness with alpha rhythm (at 45 s, C1); 2 = sleep with high-amplitude delta rhythm (at 225 s, C2); 3 = attentive alertness with dominant low-amplitude beta rhythm (500 s, PS1); 4 = active grooming or sniff-searching with theta rhythm (625 s, PS2); and 5 = the seizure state with 6–7-s SPW complexes.

Fig. 3 serves as a representative example of several other frequently observed points.

1) Almost invariably, the beginning of the seizure, as determined visually by an expert, was very precisely detected by the clustering process, as evident from a

sharp transition between different clusters. Most often, as is the case in Fig. 3, the transition was into a new cluster altogether, or even into a succession of new clusters which followed stages in the development of the seizure.

- 2) The cluster(s) which hosted the seizure was(were) the one(s) with the highest mean energy.
- 3) Sharp transitions from light sleep to an awake state were also precisely detected. A brief awakening episode (switch from cluster 2 to 1 and back) seen in Fig. 3 at 40 s, in C1, demonstrates this point.
- 4) Occasionally, epochs which were strongly clustered together with the seizure were observed prior to its ini-

TABLE I  
CLUSTER CENTERS AND STANDARD DEVIATIONS OF 13 ANIMALS. SMALL AND NEGATIVE NUMBERS ARE CAUSED BY NORMALIZATION TO ZERO MEAN AND ONE SD

CLUSTER #	SCALE 1	SCALE 2	SCALE 3	SCALE 4
1	- 0.19 ± 0.18	- 0.46 ± 0.28	- 0.73 ± 0.32	- 0.63 ± 0.22
2	0.028 ± 0.17	- 0.064 ± 0.21	- 0.068 ± 0.40	- 0.06 ± 0.17
3	0.17 ± 0.29	0.20 ± 0.35	0.35 ± 0.32	0.34 ± 0.52
4	0.32 ± 0.30	0.70 ± 0.64	1.00 ± 0.85	0.89 ± 0.85
5	2.79 ± 1.49	4.61 ± 2.77	4.50 ± 3.17	3.15 ± 1.91

TABLE II  
SUMMARY OF PIS IDENTIFICATION AND SEIZURE FORECASTING

Rat No.	Name	Seizure-time (min)	Visual signs	Optimal class No	PIS class	Definition by:	Forecasting time (min)
1	eps2	20	-	5	-	-	-
2	eps3	26	+	4	-	-	-
3	eps4	13	+	4	2,4	EE	2.5
4	eps5	9.5	+	5	4	EE+BG *	1.5
5	eps6	14.5	-	5	4	BG *	4
6	eps7	18	+	5	4,5	EE+BG	4.5
7	eps8	16	+	5	4	EE+BG	2.5
8	eps9b	55	+	8	1,2	EE+BG	2
9	eps10	14	-	5	-	-	-
10	eps11	13	-	7	5	BG	4.2
11	eps12	10	+	6	3,4	BG *	2
12	eps13	10	+	8	4	EE **	3
13	eps15	17	+	5	5	EE	4
14	eps16	9.8	+	5	5	EE	3
15	eps17	13.5	+	5	5	EE+BG	4.5
16	eps17b	10	+	4	4	EE	3
17	eps18	7	-	5	-	-	-
18	eps19	16.5	+	5	3	EE **	1.5
19	eps20	19	+	5	4	EE	0.7
20	eps21	23	+	5	4	EE	1.5
21	eps22	14.5	+	8	-	-	-
22	eps23	28	-	8	4	BG	4.2
23	eps28	53	+	5	4	EE	2.5
24	eps29	65(-)	-	4	-	-	-
25	eps32	18.5	-	8	7	EE+BG	4

PIS CLASS The cluster number(s) by which PIS was detected.

EE Epileptic events.

BG Background activity.

\* Nonspecific background alertness, mostly  $\theta$  rhythm (epochs of same class seen in other segments).

\*\* Nonepileptic events (mainly sleep spindles in the control period) included in same class.

tiation. Such epochs were seen either during the PIS (with isolated spikes or with “mini-seizures”) or else in the control period, associated with sleep patterns. In the latter case, they could easily be differentiated when considering group membership. Epoch number 6 in Fig. 3(c) is from PS2 (at 600 s) showing theta rhythm with an isolated spike. This epoch shares membership in the seizure (5) and in the active state (4) classes. Epoch number 7 is from the sleeping state (at 20 s, C1) showing an isolated sleep spindle; it shares membership in classes 5 and 2.

Table I lists the intersubject variability in the spatial position of the cluster centers of 13 animals with a five-cluster classification. It, thus, gives a measure of the signal-content uniformity and, thereby, of the universality of state classifi-

cation. To make the point, the mean ( $\pm$ SD) of four out of the eight coordinates are listed, the second-channel data being much the same.

Since on each successive cluster there is a rather uniform increase in the variances of all four scales, it would seem at first sight that classification is made according to a general increase in signal energy (amplitude). However, this is not strictly the case, as the signal’s autocorrelation coefficients hardly performed as well in defining the EEG states. Except for cluster 5, which shows significant spatial separation, there is considerable overlap of the other clusters. It is also evident that intersubject variation is quite high.

Table II is a grand summary of the exposure outcome, pattern-vector selection, cluster-number optimization, and PIS identification in all experimental animals. One can see from

the table that the optimal number of clusters (as obtained from adding one or two to the global peak of the average partition density criterion) was most frequently five, with a range from three to seven. Table II shows that in 16 out of 25 animals a PIS ranging in time between 0.7 and 4.5 min was uniquely defined, either by the appearance of a distinct new cluster, or by a new combination of membership-sharing in two or more clusters.

Fig. 4 shows a case in which the PIS was identified by a combination of nonspecific background activity and the appearance of sporadic epileptic activity. The upper panel shows the value of the average partition density Criterion computed for a 1–9 cluster partitioning. The peak at three clusters calls for an optimal partitioning to four clusters. The middle and bottom panels are the same as in Fig. 3. In the lower panel, several transitions from light sleep (class 3) to attentive wakefulness (class 1) are seen throughout. From the middle of PS1, an active awake state (class 2) appears and begins to dominate in PS2. At the same time, many single and groups of spikes, including a mini-seizure at 710 s, are evident as dense epochs in the emerging class 4, which later is seen to also include the seizure (at 760 s). Sparse epochs classified in Fig. 4 also appear in C1-P2, but always in the background of the sleeping state. From PS1 onwards, they spring from the awake and active states. A 2.5-min PIS is thereby defined.

Another glance at Table I will show that the cluster numbers which identified the PIS by the occurrence of single events are high (either the last or the last but one), signifying high-amplitude events. As mentioned earlier, the seizures proper were always contained in the highest energy cluster(s). Identification of the PIS by a change in background activity was often based on lower cluster numbers and varied between animals. An example in which the PIS is defined by a change in background activity is shown in Fig. 5. In this case, the animal was awake throughout. No visual signs of epileptic activity were observed prior to seizure onset, which occurred at 760 s, in PS2. The optimal clustering criterion called for a seven-cluster partitioning. Clusters 6 and 7, containing epochs with the highest energies are uniquely associated with the seizure. The next cluster down, number 5, which gains importance starting from the middle of PS1 and which was not associated with any distinct rhythms, clearly defines a 2-min long PIS.

In three instances the PIS was apparently defined nonspecifically, mostly as a state of dominant theta rhythm. In six animals the PIS could not be defined, as portrayed in Fig. 6.

An illustration of the dynamic version of the method is given in Fig. 7. Determining the optimal number of clusters was first performed in the manner described for all previous exposures, by presenting the UOFC with all pattern-vectors at once. A peak at 4 prompted a partitioning to five classes. Next, the evolution of the average partition density criterion value with time was followed by starting a five-cluster partitioning on 300 vectors (2.5 min) and then adding 60 vectors (0.5 min) at a time, until the final value was arrived at when all the vectors were supplied. This is shown in the upper panel of Fig. 7. The value for a five-class partitioning stays rather low and begins to climb appreciably after ten minutes. The middle panel of Fig. 7 shows the dynamic tracking of cluster-center positions

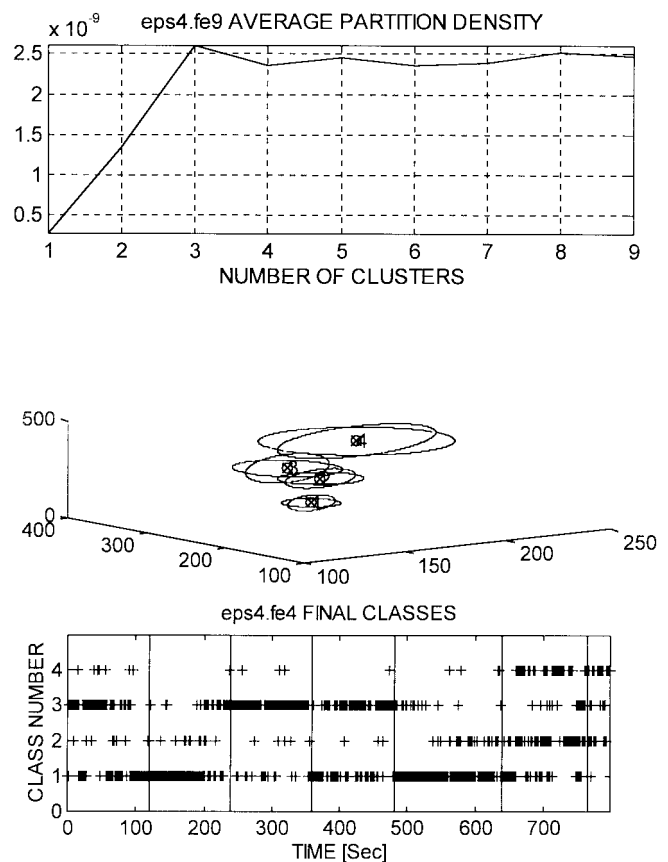


Fig. 4. PIS definition by appearance of epileptic activity. The plot in the upper panel has the average partition density criterion in the  $Y$  axis and number of clusters in the  $X$  axis. Scales of the middle and bottom panels are the same as in Fig. 3(a) and (b), respectively, but only the centers and the SD-ellipses of the point distances are shown. From the middle of S1, many single and groups of spikes, including a mini-seizure at 710 s, are evident as dense epochs with 100% membership in class 4, which later is seen to also include the seizure (at 760 s).

as time passes and consecutive epochs are added. Even in the three visible dimensions, centers 3, 4, and 5 show considerable spatial shifts, probably in correlation with the gradual establishment of a class-5 PIS at 550 s in PS1, as seen in the lower panel. The seizure started a few seconds after the end of PS2.

#### IV. DISCUSSION

The problematics of epilepsy forecasting are evident from the scarcity of works devoted to this aspect amongst the abundance of published material concerned with epileptic-pattern recognition. They stem from two main reasons.

- 1) The apparent chaotic behavior of the preepileptic state which very abruptly and unexpectedly switches into the generalized seizure. This is in marked contrast to the transition between most of the normal states, with the notable exception of sudden awakening.
- 2) When alarming single events do appear in the PIS, their templates show individual variability in both form and timing, thus, complicating supervised learning.

The method we describe, uses wavelet analysis and fuzzy clustering, both of which are efficient in unsupervised learning. Discrete clustering has been used to separate epileptic spikes

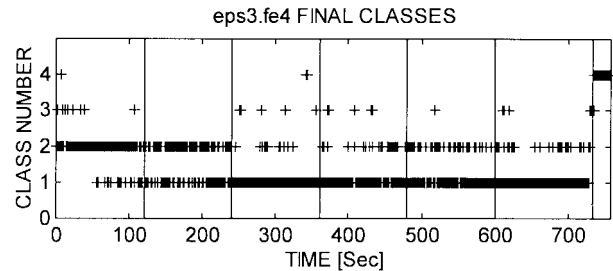
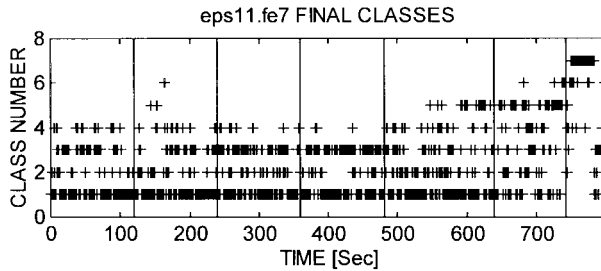
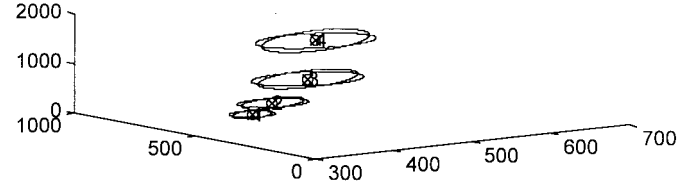
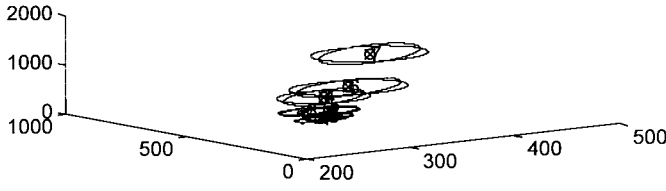
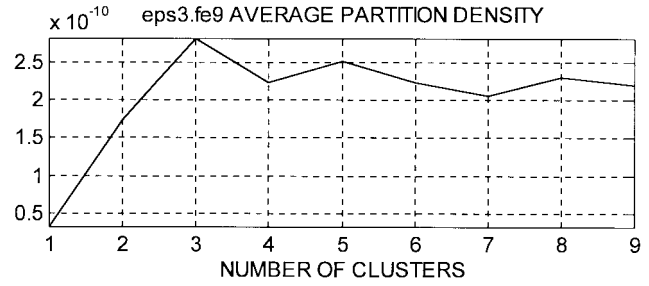
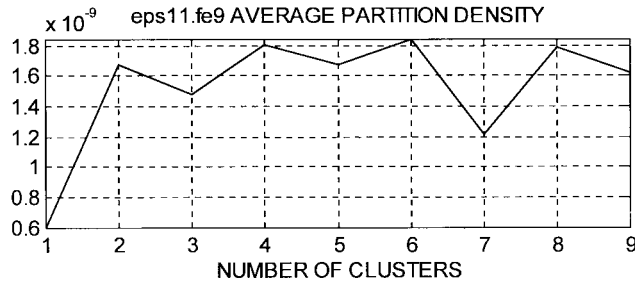


Fig. 5. PIS definition by change in background activity. Panels as in Fig. 4. Optimal partitioning to seven classes. Animal awake throughout exposure. No distinct epileptic activity seen before the seizure, at 740 s in PS2. Classes 6 and 7 are uniquely associated with the seizure. Class 5 defines the PIS very specifically, and forecasts the seizure two minutes before its onset.

Fig. 6. PIS not defined. Panels as in Fig. 5. Unanticipated seizure at 730 s, in S2.

and waves from the background activity [11], wavelet analysis has been used to extract epileptic elements for inputs to a neural network [20] and fuzzy clustering has been used in conjunction with adaptive segmentation to sort and identify epileptic transients [21]. The combination we present, specifically aimed at forecasting generalized epilepsy, has, to our knowledge, never been used before. Although intended as a forecaster, the method, in fact, turned out to be an excellent automated identifier of EEG states, including the IS which was classified as such upon the appearance of the first spike or SPW in the impulse train of the seizure. Also, isolated single epileptic events, occurring in the PIS, were readily identified, and the epochs containing them were either uniquely classified or else, jointly with the IS.

Although nonepileptic single events, such as sleep spindles and k-complexes, often caused their host epochs (usually in the preexposure control period) to be classified together with the PIS or even to be included in the seizure category (Fig. 3), they could, for the most part, be dismissed by taking account of the underlying state, since in this experimental model seizures never sprang from the sleeping state. Further separation of nonepileptic from preepileptic and epileptic epochs could be achieved by first classifying all points by one pattern vector (variance), and then trying to split “suspicious” clusters by the same or by another vector.

The suitability and effectiveness of the method as a forecaster should be assessed in terms of specificity, sensitivity, and universality. As mentioned above, specificity was rather good, especially when considering not only the predominant class of each state but also the degree of membership in each of the classes. By so doing, PIS’s of most of the animals could be uniquely defined. The wide range of seizure time lags (Table II) ensures that it is the PIS rather than a certain HBO-exposure time which is being defined. We did not have enough nonseizing animals from which to further evaluate false positives. In the one animal which did not seize, a small number of classes (three) was detected, all representing normal EEG states.

As for sensitivity, we believe that with the obvious limitations of surface recordings and the small number of electrodes, some animal’s PIS’s are bound to be missed. We have previously reported on an increase in the two-channel correlation coefficient as an identifier of the PIS in the same experimental model [38]. This forecaster was not very specific, but quite sensitive. Multichannel correlation combined with wavelet scale energy could improve this aspect. Adding other features extracted by related methods (such as the exponential distribution [19]), other central nervous system electrical activity (such as evoked potentials), and even extra-cerebral biological signals (such as heart-rate variability) as inputs to the fuzzy clustering process, could further improve sensitivity.

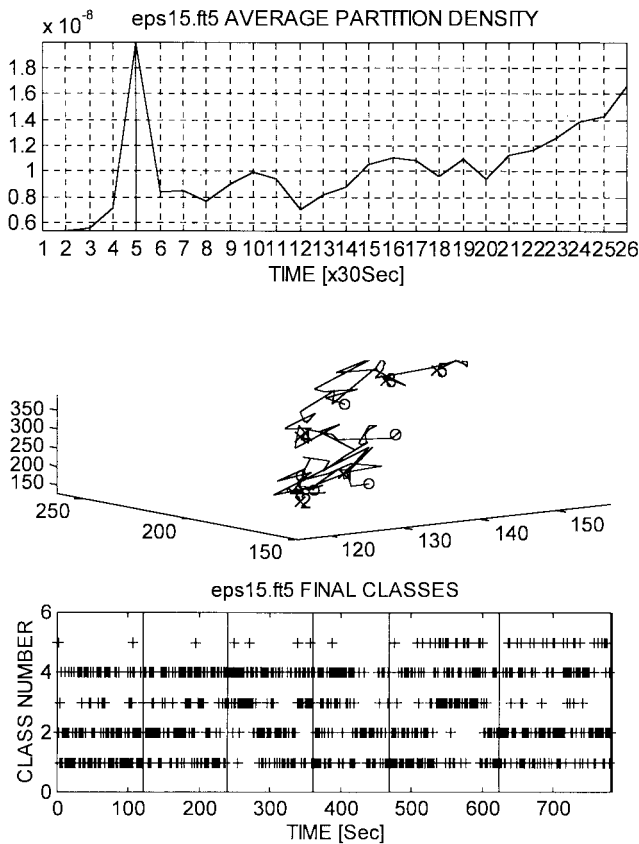


Fig. 7. Dynamic version of UOFC. (top) The evolution with time of the value of the average partition density Criterion. The X axis is a time scale with 30-s units. (middle) Scales are similar to previous figures, but the movement of each cluster center is followed after each time unit, starting at  $\circ$  and ending at  $\times$ . (bottom) Similar to previous figures, the seizure started a few seconds after the end of PS2.

The universality of the PIS, even for unrestrained rats, falls short of the expected. In the instances in which the seizure was also visually foreseen, the PIS was uniformly defined as a state of relatively high energy in all wavelet-scale transforms of the two EEG channels (Tables I and II). In the rest, no distinct change in background can as yet be associated with this state. Intersubject variability in PIS features could be circumvented by resorting to the method of dynamic tracking of the centers during the exposure and by presenting the UOFC with an expanded preexposure period in order to better establish the individual normal pattern repertoire. Dynamic clustering as presented by the example in Fig. 7 is also a step toward true forecasting in real time. Its advantage is the continuous evaluation of incoming new data in the light of the cumulative past history of a particular exposure, or any other time-series. Removing the constraint of a predetermined number of clusters, or allowing the UOFC to find the optimum number on a stretch of normal EEG, could add the emergence of a new cluster to the list of indicators of pathology. Alternatively, when enough experimental and clinical data has been processed, certain universal clusters may emerge and form the basis for supervised learning by a set of rules.

While modern notions of deep (limbic, thalamic) origins of generalized seizures [39]–[41] would suggest preferred

deep recording sites for detecting such changes, recent experimental evidence of generalized seizure initiation points to coincidental or even precedent cortical involvement [42]. The latter favor the chances of early detection from surface recording, thereby complying with the required noninvasivity of most applications.

In summary, we present a method which seems particularly suitable for an accurate and reliable identification of bioelectric states of the cerebral cortex, whether from the background EEG activity and/or from a preponderance of spontaneous single events. The method will also detect either sharp or gradual transitions between states and in some instances, as in the current example of epilepsy, may provide a timely warning for the emergence of generalized pathology, from seemingly subtle changes in the physiological state of the cortex.

At this stage, the method utilizes unsupervised fuzzy clustering which is fed very few parameters derived from feature extraction by wavelet transform of two EEG channels. Adding more channels to the feature-extracting process and more parameters, derived from other bioelectric signals, to the clustering process should increase the forecasting power of this method. Other candidates for applying the method as a warning device could be impending psychotic states—detrimental effects of hypoxia in pilots and loss of vigilance in drivers—as well as extra-cerebral pathologies such as heart attack, based on heart-rate variability.

#### APPENDIX A THE FWT

Any function  $\theta(t)$  whose integral is equal to one and that converges to zero at infinity is called a smoothing function. In our case,  $\theta(t)$  is chosen to be a Gaussian function. Let  $\psi(t)$  denote the first derivative of  $\theta(t)$  (which results in a biphasic waveform). By definition, the function  $\psi(t)$  can be considered to be wavelet because its integral is equal to zero. Let  $\psi_a(t)$  be the dilation by scaling factor  $a$  of the function  $\psi(t)$

$$\psi_a(t) = \frac{1}{a} \psi\left(\frac{t}{a}\right).$$

The wavelet transform is computed by convolving the signal  $S$  with these dilated wavelets. To allow fast numerical implementations, the scale  $s$  is varied along the dyadic sequence ( $2^j$ ). The wavelet transform  $T_{2^j}S(t)$  is defined by

$$\begin{aligned} T_{2^j}S(t) &\equiv S(t) * (2^j \psi_{2^j})(t) = S(t) * \left(2^j \frac{d\theta_{2^j}}{dt}\right)(t) \\ &= 2^j \frac{d}{dt} (S * \theta_{2^j})(t). \end{aligned}$$

The wavelet function  $\psi(t)$  can be characterized by the discrete filters,  $H$  (low-pass) and  $G$  (high-pass) [34], where the low-pass filter  $H$  is a product of the Gaussian  $\theta(t)$ , and the high-pass filter  $G$  is a product of its derivative. The discrete filters  $H_{2^j}, G_{2^j}$  can be obtained by placing  $(2^j - 1)$  zeros between each of the coefficients of the filters. The transfer function of these filters are  $H(2^j w)$  and  $G(2^j w)$ . The wavelets corresponding to each scale can be obtained by convoluting the appropriate filters. The transform of five scales of an ictal EEG epoch is shown in Fig. 1.

The discrete wavelet transform of a signal can be estimated using the FWT proposed by Mallat and Zhong [34]. At each scale  $j$  the wavelets' coefficients  $t_{2j+1}f$  and the smoothed signal  $O_{2j+1}\mathbf{S}$  for the next scale  $j+1$  are calculated. For scale zero,  $j=0$ , the signal  $\mathbf{S}$  is used as the smoothed signal. The algorithm proposed is

```

j = 0
O2j⊂ = ⊂
While (j < J)
  T2j+1⊂ = 1/λj O2j⊂* Gj
  O2j+1⊂ = O2j⊂* Hj
end

```

where  $J$  is the total number of scales and the constant  $\lambda_j$  compensates for the discretization errors.

#### APPENDIX B THE UOFC ALGORITHM

The partitioning stage [Step 2)] of the UOFC algorithm is a combination of modified fuzzy  $K$ -mean algorithm and MLE [36]. The basic fuzzy  $K$ -mean algorithm is derived from minimization, with respect to  $\mathbf{P}$ , a set of cluster centers, and  $\mathbf{U}$ , a membership matrix, of a fuzzy version of the least-squares function

$$J_q(\mathbf{U}, \mathbf{P}) = \sum_{i=1}^M \sum_{k=1}^K u_{ki}^q \cdot d^2(\mathbf{p}_k, \mathbf{x}_i)$$

where  $u_{ki}$  is the degree of membership of the data pattern  $\mathbf{x}_i$  in the  $k$ th cluster,  $\mathbf{x}_i$  in the  $i$ th (temporal) pattern, the  $i$ th column in the  $\mathbf{X}$  data matrix,  $\mathbf{p}_k$  is the center of the  $k$ th cluster,  $d^2(\mathbf{p}_k, \mathbf{x}_i)$  is the square of the distance (Euclidean or any other distance function) between  $\mathbf{x}_i$  and  $\mathbf{p}_k$ ,  $M$  is the number of data patterns, and  $K$  is the number of clusters in the current partition. The parameter  $q$  (commonly set to two) is the weighting exponent for  $u_{ki}$  and controls the "fuzziness" of the resulting clusters [36]. The basic  $K$ -mean clustering algorithm includes the following steps:

- 1) Choose primary centroids (prototypes)  $\mathbf{p}_k, k = 1, \dots, K$ .
- 2) Calculate the degree of membership  $u_{ki}$  of all data patterns in all clusters by

$$u_{ki} = \frac{\left[ \frac{1}{d^2(\mathbf{x}_i, \mathbf{p}_k)} \right]^{1/(q-1)}}{\sum_{j=1}^K \left[ \frac{1}{d^2(\mathbf{x}_i, \mathbf{p}_j)} \right]^{1/(q-1)}}$$

- 3) Calculate the new set of cluster centers from

$$\mathbf{p}_k = \frac{\sum_{i=1}^M u_{ki}^q \cdot \mathbf{x}_i}{\sum_{i=1}^M u_{ki}^q}, \quad k = 1, \dots, K.$$

- 4) If

$$\max_{k,i} [|u_{ki} - (\text{previous } u_{ki})|] > \varepsilon$$

go to Step 2).

In the UOFC a modification of this algorithm is used in two phases to account for normally distributed clusters with large variability of covariance matrix (shape, size, and density) and number of patterns. In the first phase, the fuzzy  $K$ -mean algorithm is performed with Euclidean distance function

$$d^2(\mathbf{p}_k, \mathbf{x}_i) = [(\mathbf{p}_k - \mathbf{x}_i)^T \cdot (\mathbf{P}_k - \mathbf{x}_i)].$$

The final cluster centers of the first phase are used as the initial centroids for the second phase. In the second phase, a fuzzy modification of the MLE is utilized, by using the following exponential distance function in the fuzzy  $K$ -mean algorithm:

$$d^2(\mathbf{p}_k, \mathbf{x}_i) = \frac{[\det(\mathbf{F}_k)]^{1/2}}{s_k} \cdot \exp \left[ (\mathbf{p}_k - \mathbf{x}_i)^T \cdot \mathbf{F}_k^{-1} \cdot (\mathbf{p}_k - \mathbf{x}_i) \right] \quad \text{where}$$

$$s_k = \frac{1}{M} \cdot \sum_{i=1}^M u_{ki}$$

is the sum of memberships within the  $k$ th cluster, which consist of the *a priori* probability of selecting the  $k$ th cluster and

$$\mathbf{F}_k = \frac{\sum_{j=1}^M u_{kj} (\mathbf{p}_k - \mathbf{x}_j) \cdot (\mathbf{p}_k - \mathbf{x}_j)^T}{\sum_{i=1}^M u_{ki}}$$

is the fuzzy covariance matrix of the  $k$ th cluster. By applying these two phases, the robustness of the fuzzy  $K$ -mean algorithm with the Euclidean distance function is used for finding a feasible initial partition, and the adaptiveness of the fuzzy modification of the MLE is utilized to refine the partition for a large variability of cluster shapes, densities, and number of data points in each cluster. Note that other distance functions can be used according to the intrinsic characteristic of the data.

In Step 3) the following performance measures for cluster validity are calculated:

- 1) The fuzzy hypervolume criterion is calculated by  $v_{HV}(K) = \sum_{k=1}^K h_k$ , where the hypervolume of the  $k$ th cluster is defined by  $h_k = [\det(\mathbf{F}_k)]^{1/2}$ .
- 2) The partition density is calculated by  $v_{PD}(K) = (\sum_{k=1}^K S_k / \sum_{k=1}^K h_k)$ .
- 3) The average density is calculated by  $v_{AD}(K) = (1/K) \sum_{k=1}^K (S_k / h_k)$ .

The UOFC algorithm is terminated when the performance measures for cluster validity reach their best value.

#### REFERENCES

- [1] P. Loiseau, "Epilepsies," in *Guide to Clinical Neurology*. New York: Churchill Livingstone, 1995, pp. 903–914.
- [2] G. Dumermuth, "Possibilities of electronic EEG processing in epileptology," in *Epileptology: Proc. 7th Int. Symp. on Epilepsy*, 1976. pp. 365–372.
- [3] J. M. Clark, "Oxygen toxicity," in *The Physiology and Medicine of Diving*, 3rd ed. San Pedro, CA: Best, 1978, pp. 200–238.

- [4] F. H. Lopes da Silva, J. P. Pijn, and D. N. Velí, "Signal processing of EEG: evidence for chaos or noise. An application to seizure activity in epilepsy," in *Advances in Processing and Pattern Analysis of Biological Signals*. New York: Plenum, 1996, pp. 21–32.
- [5] J. R. G. Carrié, "A hybrid computer system for detecting and quantifying spike and wave EEG patterns," *Electroencephalogr. Clin. Neurophysiol.*, vol. 33, pp. 339–341, 1972.
- [6] E. E. Gose, S. Werner, and R. C. Bickford, "Computerized EEG spike detection," in *Proc. San Diego Biomed. Symp.*, vol. 13, pp. 193–198, 1974.
- [7] J. R. Smith, "Automatic analysis and detection of EEG spikes," *IEEE Trans. Biomed. Eng.*, vol. BME-21, pp. 1–7, 1974.
- [8] A. S. Gevins, C. L. Yeager, S. L. Diamond, G. M. Zeitlin, J. P. Spire, and A. H. Gevins, "Sharp-transient analysis and threshold linear coherence spectra of paroxysmal EEG's," in *Quantitative Analytic Studies in Epilepsy*. New York: Raven, 1976, pp. 463–481.
- [9] F. H. Lopes da Silva, W. ten Broeke, K. van Hulten, and J. G. Lommen, "EEG nonstationarities detected by inverse filtering in scalp and cortical recordings of epileptics: Statistical analysis and spatial display," in *Quantitative Analytic Studies in Epilepsy*. New York: Raven, 1976, pp. 375–387.
- [10] J. Gotman and P. Gloor, "Automatic recognition and quantification of interictal epileptic activity," *Electroenceph. Clin. Neurophysiol.*, vol. 4, pp. 513–529, 1976.
- [11] K. M. Ma, G. G. Celesia, and W. P. Birkemeier, "Cluster analysis and spike detection in EEG," in *Epileptology: Proc. 7th Int. Symp. on Epilepsy*, 1976, pp. 386–396.
- [12] W. P. Birkemeier, A. B. Fontaine, G. G. Celesia, and K. M. Ma, "Pattern recognition techniques for the detection of epileptic transients of EEG," *IEEE Trans. Biomed. Eng.*, vol. BME-25, pp. 213–217, 1978.
- [13] J. D. Frost, Jr., "Automatic recognition and characterization of epileptiform discharges in the human EEG," *J. Clin. Neurophysiol.*, vol. 2, pp. 231–249, 1985.
- [14] A. Babloyantz and A. Destexhe, "Low dimensional chaos in an instance of epilepsy," *Proc. Nat. Acad. Sci. USA*, vol. 83, pp. 3513–3517, 1986.
- [15] P. E. Rapp, "Oscillations and chaos in cellular metabolism and physiological systems," in *Chaos-Nonlinear Science: Theory and Applications*. Manchester, U.K.: Manchester Univ. Press, 1986, pp. 179–208.
- [16] J. Gotman and L. Y. Wang, "State-dependent spike detection: Concepts and preliminary results," *Electroencephalogr. Clin. Neurophysiol.*, vol. 79, pp. 11–19, 1991.
- [17] A. P. Pijn, J. Van Neerven, N. Noestt, and F. H. Lopes Da Silva, "Chaos or noise in EEG signals: Dependence on state and brain site," *Electroencephalogr. Clin. Neurophysiol.*, vol. 79, pp. 371–381, 1991.
- [18] T. F. Collura, H. H. Morris, M. D. Burgess, M. D. Jacobs, and G. H. Klemm, "Phase-plane trajectories of EEG seizure patterns in epilepsy," *Amer. J. EEG Technol.*, vol. 32, pp. 295–307, 1992.
- [19] W. J. Williams, H. P. Zaveri, and J. C. Sackellares, "Time-frequency analysis of electrophysiology signals in epilepsy," *IEEE Eng. Med., Biol. Mag.*, vol. 14, pp. 123–143, 1995.
- [20] T. Kalayci and Ö. Özdamar, "Wavelet preprocessing for automated neural network detection of EEG spikes," *IEEE Eng. Med., Biol. Mag.*, vol. 14, pp. 160–166, 1995.
- [21] V. Krajca, S. Petranek, I. Patakova, and A. Varri, "Automatic identification of significant graphoelements in multichannel EEG recordings by adaptive segmentation and fuzzy clustering," *Int. J. Biomed. Comput.*, vol. 28, pp. 71–89, 1991.
- [22] N. Radaý, N. Conforty, D. Harel, and S. Lavy, "Analysis of pre-seizure electrocorticographic changes in rats during hyperbaric oxygenation," *Exp. Neurol.*, vol. 46, pp. 9–19, 1975.
- [23] D. O. Walter, "Recent Applications of EEG analysis to epilepsy," in *Epileptology: Proc. 7th Intl. Symp. Epilepsy*, 1976, pp. 372–376.
- [24] Z. Rogowski, I. Gath, and E. Bental, "On the prediction of epileptic seizures," *Biol. Cybern.*, vol. 42, pp. 9–15, 1981.
- [25] D. Torbati, A. J. Simon, and A. Ranade, "Frequency analysis of EEG in rats during the preconvulsive period of O<sub>2</sub> poisoning," *Aviat. Space Environ. Med.*, vol. 52, pp. 598–603, 1981.
- [26] P. Guedes de Oliveira, C. Queiroz, and F. H. Lopez da Silva, "Spike detection based on a pattern recognition approach using a microcomputer," *Electroencephalogr. Clin. Neurophysiol.*, vol. 56, pp. 97–103, 1983.
- [27] L. D. Iasemidis and J. C. Sackellares, "The evolution with time of the spatial distribution of the largest Lyapunov exponent the human epileptic cortex," in *Measuring Chaos in the Human Brain*, D. Duke and W. Pritchard, Eds. Singapore: Singapore World Scientific, 1991, pp. 49–82.
- [28] I. Gath, C. Feuerstein, D. T. Pham, and G. Rondouin, "On the tracking of rapid dynamic changes in seizure EEG," *IEEE Trans. Biomed. Eng.*, vol. 39, pp. 952–958, 1992.
- [29] I. Gath, B. Harris, Y. Salant, C. Feuerstein, O. Henriksen, and G. Rondouin, "Processing of epileptic EEG," in *Advances in Processing and Pattern Analysis of Biological Signals*. New York: Plenum, 1996, pp. 57–70.
- [30] I. Gath, C. Feuerstein, and A. Geva, "Unsupervised classification and adaptive definition of sleep patterns," *Pattern Recogn. Lett.*, vol. 15, pp. 977–984, 1994.
- [31] I. Gath and A. Geva, "Unsupervised optimal fuzzy clustering," *IEEE Trans. Pattern Anal. Machine Intell.*, vol. 7, pp. 773–781, 1989.
- [32] ———, "Fuzzy clustering for estimation of parameters of the components of mixtures of normal distributions," *Pattern Recogn. Lett.*, vol. 9, pp. 77–86, 1989.
- [33] S. G. Mallat and S. Zohng, "Matching pursuits with time-frequency dictionaries," *IEEE Trans. Signal Processing*, vol. 12, pp. 3397–3415, 1993.
- [34] ———, "Characterization of signal from multiscale edges," *IEEE Trans. Pattern Anal. Machine Intell.*, vol. 10, pp. 710–732, 1992.
- [35] M. Sun and R. J. Scwabassi, "Wavelet feature extraction from neurophysiological signals," in *Contribution to Time-Frequency and Wavelet Transforms in Biomedicine*, M. Akay, Ed. Piscataway, NJ: IEEE Press.
- [36] J. C. Bezdek, *Pattern Recognition with Fuzzy Objective Function Algorithms*. New York: Plenum, 1981.
- [37] A. Geva and H. Pratt, "Unsupervised clustering of evoked potentials by waveform," *Med., Biol. Eng., Comput.*, vol. 32, pp. 543–550, 1994.
- [38] D. Kerem and A. Geva, "Forecasting CNS-oxygen-toxicity in the rat from changes in EEG auto and cross-correlation," in *Proc. XVIIIth Annu. Meeting Eur. Undersea Biomed. Soc. Foundation for Hyperbaric Medicine*, 1992, pp. 109–111.
- [39] M. Inoue, J. Duysens, J. M. Vossen, and A. M. Coenen, "Thalamic multiple-unit activity underlying spike-wave discharges in anesthetized rats," *Brain Res.*, vol. 612, pp. 35–40, 1993.
- [40] G. V. Walenstein, "The role of thalamic IGABAB in generating spike-wave discharges during petit mal seizures," *Neuroreport.*, vol. 5, pp. 1409–1412, 1994.
- [41] M. Velasco, F. Velasco, H. Alcalá, G. Davila, and A. E. Diaz-de-Leon, "Epileptiform EEG activity of the centromedian thalamic nuclei in children with intractable generalized seizures of the Lennox-Gastaut syndrome," *Epilepsia*, vol. 32, pp. 310–321, 1991.
- [42] D. Contreras and M. Steriade, "Relations between cortical and thalamic cellular events during transitions from sleep patterns to paroxysmal activity," *J. Neurosci.*, vol. 15, pp. 623–642, 1995.



**Amir B. Geva** (S'89–M'97) was born in Haifa, Israel, in 1959. He received the B.Sc. degree (1981) in computer engineering, the M.Sc. degree (1987) on optimal fuzzy partition of sleep EEG, and the D.Sc. degree (1994) on spatio-temporal source estimation of human evoked potentials, in biomedical engineering, all from the Technion—Israel Institute of Technology, Haifa.

His research interests include: biomedical signal (EEG, heart rate variability, and blood flow sound) processing and system modeling, algorithms and computer systems, pattern recognition, fuzzy clustering, neural networks, wavelets analysis, time-series prediction, bioelectric inverse problem, and functional brain imaging and modeling.



**Dan H. Kerem** was born in 1941 in Jerusalem, Israel. He received the B.Sc. degree in biology (1961) and the M.Sc. degree in physiology (1963) on blood acidity effects on the EEG of the isolated brain, from the Hebrew University in Jerusalem, and the Ph.D. degree in diving physiology (1971) on the tolerance of the seal's brain to hypoxia, from the University of California at San Diego (UCSD), La Jolla.

Retired, he was Head of Research at the Israeli Naval Medical Institute. His longtime interest in forecasting brain oxygen toxicity spurred his recent involvement in the use of time-frequency analysis and fuzzy clustering on EEG and heart-rate variability, for the early prediction of brain state transitions.